Kinetics and equilibrium adsorption studies of dimethylamine (DMA) onto ion-exchange resin

Qinhai Hu [a,*], Yuanyuan Meng [a], Tongxi Sun [b], Qaisar Mahmood [c], Donglei Wu [a], Jianhang Zhu [a], George Lu [d]

[a] College of Environmental and Resources Science, Zhejiang University, Hangzhou 310029, Zhejiang, China
[b] College of Biological and Environmental Engineering, Zhejiang University of Technology, Hangzhou 310032, China
[c] Department of Environmental Sciences, COMSATS University, Abbottabad 22060, Pakistan
[d] Golden Maple Leaf Corporation of Hangzhou, Hangzhou 310012, China

ARTICLE INFO

ABSTRACT

The fine grained resin ZGSPC106 was used to adsorb dimethylamine (DMA) from aqueous solution in the present research. Batch experiments were performed to examine the effects of initial pH of solution and agitation time on the adsorption process. The thermodynamics and kinetics of adsorption were also analyzed. The maximum adsorption was found at natural pH of DMA solution and equilibrium could be attained within 12 min. The equilibrium adsorption data were conformed satisfactorily to the Langmuir equation. The evaluation based on Langmuir isotherm gave the maximal static saturated adsorption capacity of 138.89 mg/g at 293 K. Various thermodynamic parameters such as free energy (ΔG°), enthalpy (ΔH°) and entropy (ΔS°) showed that the adsorption was spontaneous, endothermic and feasible. DMA adsorption on ZGSPC106 fitted well to the pseudo-second-order kinetic model. Furthermore, the adsorption mechanism was discussed by Fourier transform infrared spectroscopy (FT-IR) analysis.

1. Introduction

N,N-dimethylformamide (DMF) is widely used as solvent during the polyurethane (PU) synthetic leather production, and is generally sent to the distillation process for recovery [1]. However, it can result in the generation of wastewater containing dimethylamine (DMA) as much as several hundred or thousands milligrams per liter in the top of distillation towers [2]. Apart from that, DMA also occurs in wastewater coming from pesticides, pharmaceuticals and rubber industries with DMA as their important raw material [3]. Wastewater containing DMA produces pungent odor that may cause serious pollution to the air and water resources if untreated. Since environmental pollution is becoming increasingly serious now, effective and economic removal of DMA from wastewater is a crucial research topic.

In general, the most commonly employed methods to treat DMA containing wastewaters are rectification and air rectification owing to the low boiling point of DMA (only 6.9 °C at normal temperature and pressure) [2,4]. However, both the methods primarily fit for wastewater of extremely high concentration (usually tens of thousands milligrams per liter) and both need large investment and high energy consumption. Other methods include complex extraction, liquid membrane separation, resin adsorption and so forth [5–7]. In recent years, the resin adsorption has received more attention and seems to be the most suitable option for the treatment of DMA wastewater in case of not extremely high concentration on account of its low cost and high efficiency [8]. Pan [9] investigated the sorption of DMA on weak-acid cation exchange resin D113. Results showed that the removal rate reached 91.5% and the regeneration rate was above 90% under the optimal conditions. Geng [10] observed that a strong-acid cation exchange resin 001×7 had a good sorption ability for DMA and the statically saturated sorption capacity was 107 mg/g. Informed researches focus on disposing DMA wastewater of low-concentration (<500 mg/L), and the resins mostly used have relatively large particles; whereas fine grained resins with greater specific surface area will have higher absorption capacity [11,12] and can be expected to deal with wastewater containing higher DMA concentrations.

The specific objective of the present study was to investigate the potential of fine grained resin ZGSPC106 for DMA adsorption from aqueous solution in batch experiments. The adsorption kinetics, thermodynamics and optimum reaction conditions were also investigated. Furthermore, the adsorption mechanism was discussed by infrared spectroscopy.

---

* Corresponding author. Tel.: +86 571 86971160; fax: +86 571 86971160.
E-mail address: qhhu@zju.edu.cn (Q. Hu).

Table 1
Characteristics properties of the ZGSPC106 resin.

Type	Strong acid cation resin
Matrix	Styrene–divinylbenzene
Structure	Gel type
Functional groups	–SO₃H
Particle size range (mm)	0.200–0.315
Moisture holding capacity (%)	52.0–57.0
Total exchange capacity (mmol/g)	≥4.50

2. Experimental

2.1. Materials

The resin used in the experiments was ZGSPC106 (provided by the Hangzhou Zhengguang Resin Plant, China) and its physical properties were shown in Table 1. The 33% solution of DMA (purchased from Shanghai SSS Reagent Co., Ltd, China) was diluted as required to obtain DMA solutions containing 800–2200 mg/L. Deionized water was used for all dilutions and the other reagents including NaCl, HCl and NaOH (all purchased from Sinopharm Chemical Reagent Co., Ltd, China) were of analytical reagent grade.

2.2. Analytical procedures

Concentration of DMA in solution was determined with UV-2802 spectrophotometer (Unico Instrument Co., Ltd, China) at λ_{max} = 585 nm [13], and pH was measured by PHS-3B precise pH meter (Shanghai Precision & Scientific Instrument Co., Ltd, China). Ion exchange experiments were carried out in the HZ-9211K thermostat shaker (Jiangsu Taicang Laboratorial Equipment Factory, China), and Nicolet 6700 FT-IR spectrometer (Thermo Nicolet Scientific LLC, America) was used for the adsorption mechanism analysis.

2.3. Static equilibrium adsorption experiment

Prior to use, the resins should be sequentially dipped in double volumes of 10% sodium chloride solution, 1 mol/L sodium hydroxide and 1 mol/L hydrochloric acid for 24 h [14]. Then the resins were washed with deionized water repeatedly and dried in vacuum oven at 50 °C to constant weight. The batch experiments were conducted in air tight conical flasks. Each time, 0.5 g dry resin and 50 mL DMA solution were added, and then shaken in a thermostat shaker at 160 rpm for a predetermined period.

Adsorption isotherm study was carried out with different initial DMA concentrations (800–2200 mg/L) at different temperatures (20, 40 and 60 °C). The pH was not adjusted, and the equilibrium time was set as 30 min (found out from the kinetic studies). Afterwards, samples were separated by filtration and the DMA concentrations were analyzed by spectrophotometer. In pH studies, 1 mol/L sodium hydroxide or 1 mol/L hydrochloric acid was used to adjust sample pH with initial DMA concentrations of 800 and 1000 mg/L. The adsorption capacity at equilibrium, Q_e (mg/g) was calculated by the following equation:

$$Q_e = \frac{V(C_o - C_e)}{W} \tag{1}$$

where C_o and C_e (mg/L) were the initial and equilibrium DMA concentrations in solution respectively; V (L) was the volume of the solution, and W (g) was the weight of the adsorbent.

2.4. Kinetics experiment

Kinetic experiments were performed by using 50 mL DMA solution and 0.5 g dry resin at 20 °C. The initial DMA concentration of solution was 2000 mg/L without any pH adjustment. Samples were taken at different intervals until the adsorption reached at equilibrium. The instantaneous adsorption capacity at time t, Q_t (mg/g), was obtained as follows:

$$Q_t = \frac{V(C_o - C_t)}{W} \tag{2}$$

where C_t (mg/L) was the DMA concentration in solution at time t.

2.5. Theory of adsorption

2.5.1. Adsorption isotherms

For further analysis of adsorption mechanism, two widely used models, Langmuir and Freundlich [15,16] were applied to fit the experimental data. Langmuir and Freundlich models are represented as under respectively:

$$\frac{C_e}{Q_e} = \frac{C_e}{Q_m} + \frac{1}{K_L Q_m} \tag{3}$$

$$\ln Q_e = \ln K_f + \frac{1}{n} \ln C_e \tag{4}$$

where C_e (mg/L) is the equilibrium adsorbate concentration in solution, Q_e (mg/g) is the equilibrium adsorption capacity, Q_m (mg/g) is the maximal adsorption capacity, and K_L (L/mg) is a constant related to the energy of adsorption. In Freundlich isothermal equation, K_f and n are constants related to adsorption capacity and adsorption intensity, respectively.

2.5.2. Adsorption thermodynamics

Thermodynamic parameters such as Gibbs free energy change (ΔG°), enthalpy change (ΔH°) and entropy change (ΔS°) have been determined according to the following equations:

$$\ln K_d = \frac{\Delta S^\circ}{R} - \frac{\Delta H^\circ}{RT} \tag{5}$$

$$\Delta G^\circ = \Delta H^\circ - T \Delta S^\circ \tag{6}$$

$$K_d = \frac{(C_o - C_e)V}{C_e W} \tag{7}$$

where R [8.314 J/(mol K)] is the gas constant, T (K) is the absolute temperature, and K_d (L/g) is the distribution coefficient. Values of ΔH° and ΔS° can be calculated from the slope and the intercept of the plot between $\ln K_d$ versus $1/T$.

2.5.3. Adsorption kinetics

In this study, the pseudo-first-order model and the pseudo-second-order model, which are extensively used in kinetic studies, were applied to fit with the kinetics data so as to clarify the DMA adsorption kinetics onto ZGSPC106 resin.

The pseudo-first-order model can be expressed as [17]:

$$\ln(Q_e - Q_t) = \ln Q_e - K_1 t \tag{8}$$

The pseudo-second-order model can be expressed as [18]:

$$\frac{t}{Q_t} = \frac{1}{K_2 Q_e^2} + \frac{t}{Q_e} \tag{9}$$

where K_1 is the first-order rate constant (1/min), and K_2 is the second-order rate constant [g/(mg min)]. Plotting the left part of each equation against "t" can obtain K_1, K_2 and Q_e values from the slope and intercept.

3. Results and discussion

3.1. FT-IR analysis

The FT-IR spectroscopy was used to study the adsorption mechanism. Fig. 1 shows the IR spectra of ZGSPC106 resin before and after
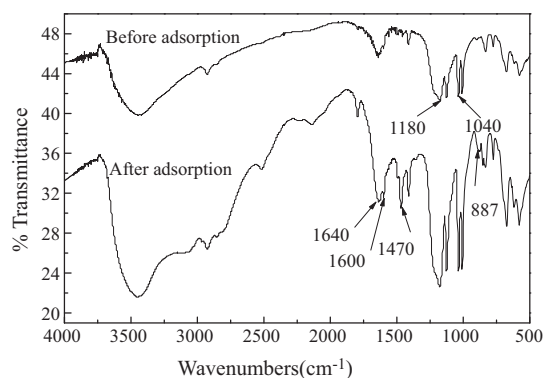
Fig. 1. FT-IR spectra of ZGSPC106 resin before and after adsorption of DMA.

DMA adsorption. The peaks observed at 1180 cm^{-1} and 1040 cm^{-1} were due to the sulfonic acid group (–SO$_3$H) of the adsorbent [19] as a kind of strong-acid cation exchange resin. After adsorption, the peaks at 1640 cm^{-1} and 887 cm^{-1} were attributed to flexure vibration and wagging vibration of –NH group while peaks at 1600 cm^{-1} might be assigned to the bending vibration of –NH$_2^+$ group. Besides, the peaks of stretching vibration of C–N group were observed at 1000 cm^{-1} and peaks at 1470 cm^{-1} were attributed to the methyl group (–CH$_3$). Therefore, it was reasonable to consider that DMA [(CH$_3$)$_2$NH], or rather DMA cations [(CH$_3$)$_2$NH$_2^+$] were introduced to the surface of the ZGSPC106 resin [20,21]. Similar results were reported for adsorption of DMA onto the 001 × 7 resin [10].

3.2. Effect of initial DMA concentration

Initial DMA concentration was adjusted in the ranges of 800–2200 mg/L for adsorption on the ZGSPC106 resin under natural pH at 20 °C for 30 min. As shown in Fig. 2, the adsorption capacity increased with increasing initial DMA concentration, however, the removal rate decreased. In the range of 800–1500 mg/L, the adsorption capacity of ZGSPC106 increased rapidly, while it increased slowly with continued increase in the DMA concentration. At the concentrations of 800 and 1000 mg/L, DMA in the solution would interact with the binding sites and thus facilitated nearly 100% adsorption for the adsorbent. With increasing concentration, there was an increase in the amount of DMA adsorbed due to increasing driving force towards the active sites on the adsorbents. At higher concentrations, a slower increase in adsorption capacity followed as the available adsorption sites gradually saturated, as a consequence more DMA was left unadsorbed. Owing to the saturation of binding sites, the adsorption capacity kept stable at about 135 mg/L and the removal of DMA has dropped to 61.1%.
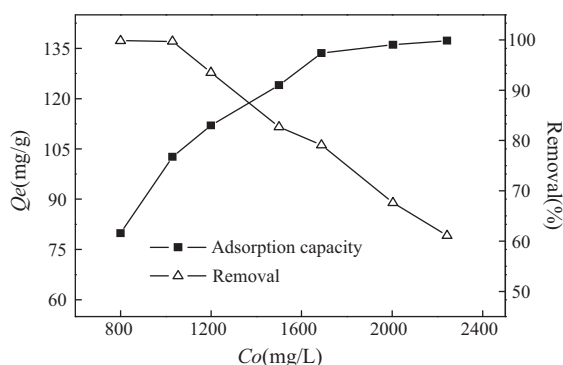

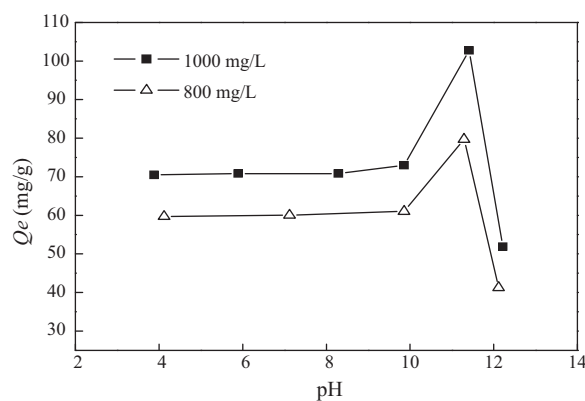**Fig. 2.** Effect of initial concentration on the adsorption of DMA by ZGSPC106.

Fig. 3. Effect of pH on the DMA adsorption with the maximum adsorption occurred at natural pH.

3.3. Effect of pH

The pH is one of the most important factors controlling the adsorption process because of its effect on the surface charge of the adsorbent as well as the degree of ionization of the adsorbate. The effect of pH on the DMA adsorption by ZGSPC106 is shown in Fig. 3 at fixed initial DMA concentrations of 800 and 1000 mg/L. For DMA solution of different concentrations, the pH had basically similar influence on the adsorption process and optimal uptake of DMA was obtained at initial pH of 11.3 and 11.4, the natural pH for DMA solution of 800 and 1000 mg/L, respectively. At initial pH lower than natural pH, a significant reduction in the DMA adsorption might probably be due to the increase of H$^+$ leading to competitive adsorption with DMA [22] or desorption of DMA from resin [23]. The minimum adsorption (about half of the maximum) occurred at initial pH value greater than natural pH indicating sodium hydroxide had more severe effect than hydrochloric acid. Similar results were obtained in the study of Geng [10]. A low DMA uptake at high pH of 12.2 probably owing to the fact that an excess of hydroxyl ions moved the hydrolytic equilibrium of DMA [4] which reduced the proportion of DMA in the available form. Furthermore, the competitive adsorption caused by addition of Na$^+$ might also account for the sharp decrease [18]. Considering the optimal uptake of DMA in solution occurred at its natural pH, all experiments in the present study were conducted without adding sodium hydroxide or hydrochloric acid for pH adjustment.

3.4. Determination of equilibrium time

Fig. 4 shows the effect of contact time on the DMA adsorption on ZGSPC106 at initial DMA concentration of 2000 mg/L. The DMA
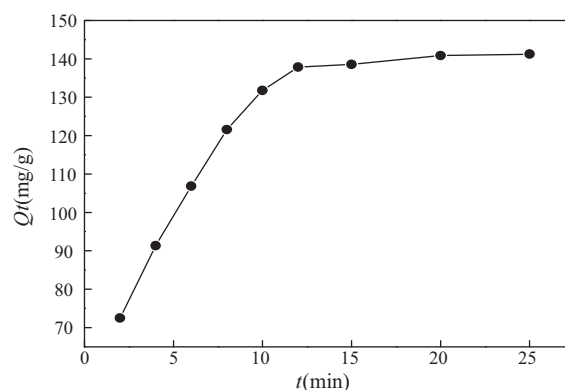

Fig. 4. Effect of contact time on the adsorption.

Table 2
Langmuir and Freundlich parameters for the DMA adsorption on ZGSPC106 resin.

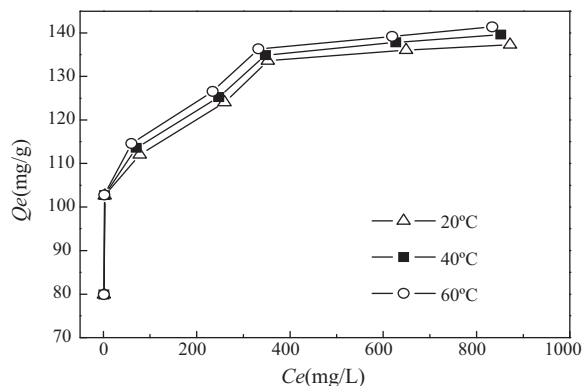| T (°C)	Total exchange capacity (mg/g)	Langmuir constants			Freundlich constants		
		Q_m (mg/g)	K_L (L/mg)	R^2	n	K_f (L/mg)	R^2
20	≥207.36	138.89	0.0906	0.9991	13.889	0.0849	0.9073
40		140.85	0.0908	0.9990	13.812	0.0860	0.9091
60		142.85	0.0958	0.9991	13.495	0.0863	0.8941

Fig. 5. Isothermal curves of adsorption.

uptake increased with the lapse of time. High adsorption rates were observed within the first 8 min, whereby over 85% of equilibrium adsorption capacity was attained. This may be due to the existence of adequate accessible resin sites available for the DMA adsorption. Further increase in contact time had a negligible effect on adsorption after 12 min which could be presumed to represent the equilibrium time. Such a short time period required to attain equilibrium suggested an excellent affinity of the adsorbent to DMA in aqueous solution. In order to ensure complete adsorption, all the experiments were conducted for 30 min.

3.5. Adsorption isotherms

The adsorption isotherm indicates the relationship between equilibrium adsorption capacity and equilibrium concentration of DMA at constant temperature. Equilibrium studies for DMA were performed by using various concentrations (800, 1000, 1200, 1500, 1700, 2000, 2200 mg/L). Fig. 5 presents the adsorption isotherms of DMA on ZGSPC106 resin at 20, 40 and 60 °C. It was observed that the DMA adsorption was higher for greater initial concentration and the equilibrium adsorption capacity increased with the rise of temperature, indicating the process to be endergonic in nature.

The Langmuir and Freundlich adsorption constants evaluated from isotherms and their correlation coefficients were presented in Table 2. It was clear that the Langmuir isotherm model provided preferable fit to the equilibrium adsorption data with correlation coefficients all close to 0.999 at different temperatures. Moreover, the values of Q_m at three different temperatures were all close to 140 mg/g, resulting in a total exchange capacity close to 70%. Since the Langmuir model is based on assumption that uniform adsorption energies distribute onto the surface and the maximum adsorption depends on saturation level of monolayer [24,25], the

DMA adsorption on ZGSPC106 resin can be reckoned as monolayer adsorption. The essential feature of Langmuir isotherm can be expressed in terms of a dimensionless separation factor, R_L, defined as [26]:

$$R_L = \frac{1}{1 + K_L C_o} \tag{10}$$

The value of R_L indicated the shape of the isotherm to be unfavorable ($R_L > 1$), linear ($R_L = 1$), favorable ($0 < R_L < 1$), or irreversible ($R_L = 0$). R_L values were found to be between 0 and 1 for all the concentrations of DMA in this study, indicating favorable DMA adsorption on ZGSPC106 resin.

3.6. Thermodynamics of DMA adsorption

The adsorption thermodynamics were studied to gain an insight into the adsorption behavior. Thermodynamic parameters are listed in Table 3. The positive $\Delta H°$ value indicated that the adsorption process was endothermic and higher temperature was conducive to the adsorption. Negative values of $\Delta G°$ revealed the spontaneous nature of adsorption. The $\Delta S°$ value was positive suggesting the increasing randomness at the solid/liquid interface during the adsorption and reflected the affinity of the adsorbent for DMA.

3.7. Kinetics of DMA adsorption

Information on the adsorption kinetics describing the solute uptake rate, which in turn governs the residence time for adsorption reaction, is one of the important characteristics defining the efficiency of adsorption. The half-adsorption time is the time required to uptake half of the maximal amount of adsorbate at equilibrium. It characterizes the adsorption rate as well. In case of pseudo-second-order process, its value is given below [27]:

$$t_{1/2} = \frac{1}{k_2 Q_e} \tag{11}$$

The calculated results are presented in Table 4. The values of correlation coefficient indicated a more satisfactory fit of pseudo-second-order model with the experimental data compared to the pseudo-first-order model. Additionally, the value of Q_e calculated from the second-order kinetic model was in better agreement with the experimental value, and therefore the pseudo-first-order model was applicable to the DMA adsorption process on ZGSPC106 resin. This can be explained by the conclusion that the pseudo-second-order model was suitable for the adsorption of lower molecular weight adsorbates on small-sized adsorbent particles, which was pointed out by Wu et al. [28].

Table 3
The adsorption thermodynamic parameters.

T (°C)	K_d	$\Delta G°$ (kJ/mol)	$\Delta H°$ (kJ/mol)	$\Delta S°$ [J/(mol K)]
20	3.51	−8.55	7.95	56.30
40	3.72	−9.67		
60	3.90	−10.80		

Table 4
Kinetic parameters for the adsorption of DMA on resin.

Pseudo-first-order			Pseudo-second-order			
K_1 (1/min)	$Q_{e,cal}$ (mg/g)	R^2	K_2 [g/(mg min)]	$Q_{e,cal}$ (mg/g)	$t_{1/2}$ (min)	R^2
0.1722	80.39	0.9275	0.0026	158.73	2.423	0.9968

4. Conclusions

This study focused on the DMA adsorption onto ZGSPC106 cation exchange resin from aqueous solution. The adsorption was found to be pH dependent and the optimum DMA adsorption occurred at natural pH of DMA solution with a maximal static saturated adsorption capacity of 138.89 mg/g (dry resin) at 20 °C. Under the studied conditions, thermodynamic calculations showed the feasibility, endothermic and spontaneous nature of the adsorption and the equilibrium data could preferably be modeled with the Langmuir isotherm. The kinetics of the adsorption followed the pseudo-second-order model. The resin has high adsorption rate for DMA since over 85% of the total adsorption was achieved during the first 8 min and equilibrium was attained within 12 min. The ZGSPC106 cation exchange resin has relatively efficient DMA adsorption capability and can be expected to remove DMA from aqueous solutions.

References

[1] S.H. Zhao, X.J. Song, N. Pei, J.Z. Zhang, S.Q. Liu, Recovery technology of DMF from wet type polyurethane synthetic leather waste gas, Chin. J. Chem. Eng. 16 (2008) 461–464.
[2] Q.L. Chang, Q.S. Li, B.H. Wang, Study on recycling and reusing of industrial wastewater containing dimethylamine, Chin. J. Environ. Eng. 4 (2010) 35–38.
[3] X.Y. You, Present situation of technology and development for methylamine and N,N-dimethylfomanide synthesis, Chem. Int. 12 (2005) 5–7.
[4] J.Z. Chen, J.X. Qu, F. He, J.Z. Yang, Study on the new technology for recovery of dimethylamine from DMF distillery wastewater in tennery factories, Ind. Saf. Environ. Prot. 35 (2009) 28–29.
[5] F.Y. Wei, J. Geng, L. Zhang, Treatment of dimethylamine wastewater by complex extraction, Chin. J. Appl. Chem. 25 (2008) 1213–1216.
[6] J.A. Lu, H.M. Song, Application of liquid membrane in treatment of organic waste water, Jiangsu Chem. Ind. 29 (2001) 29–31.
[7] J.X. Qu, J.Z. Chen, The research progress of dimethylamine wastewater by physic-chemical method, West Leather 31 (2009) 38–41.
[8] Z.F. Xie, Y. Chen, Y.J. Dai, et al., Adsorption of sulfosalicylic acid on 717 anion exchange resin, Chin. J. Process Eng. 7 (2007) 278–282.
[9] G.F. Pan, Study on the Separation of Low-concentration Dimethylamine from Wastewater of Synthetic Leather Industry, Hefei Univ. Technol., 2009.
[10] J. Geng, Treatment of the Dimethylamine Wastewater by Complex Extraction and Ion-exchange, Hefei Univ. Technol., 2009.
[11] C.K. Jain, D.C. Singhal, M.K. Sharma, Adsorption of zinc on bed sediment of river hindon: adsorption models and kinetics, J. Hazard. Mater. 114 (2004) 231–239.
[12] M. Dogan, H. Abak, M. Alkan, Adsorption of methylene blue onto hazelnut shell: kinetics, mechanism and activation parameters, J. Hazard. Mater. 164 (2009) 172–181.
[13] H.Z. Tang, Measure the concentration of dimethylamine in wastewater by spectrophotometry, Environ. Prot. Chem. Ind. 13 (1993) 371–373.
[14] F. Wang, L.J. Wang, J.S. Li, X.Y. Sun, W.Q. Han, Adsorption behavior and mechanism of cadmium on strong-acid cation exchange resin, Trans. Nonferr. Met. Soc. China 19 (2009) 740–744.
[15] S. Meenakshi, N. Viswanathan, Identification of selective ion-exchange resin for fluoride sorption, J. Colloid Interface Sci. 308 (2007) 438–450.
[16] J. Anandkumar, B. Mandal, Removal of Cr(VI) from aqueous solution using Bael fruit (Aegle marmelos correa) shell as an adsorbent, J. Hazard. Mater. 168 (2009) 633–640.
[17] Q.S. Liu, T. Zheng, P. Wang, J.P. Jiang, N. Li, Adsorption isotherm, kinetic and mechanism studies of some substituted phenols on activated carbon fibers, Chem. Eng. J. 157 (2010) 348–356.
[18] X. Yang, B. Al-Duri, Kinetic modeling of liquid-phase adsorption of reactive dyes on activated carbon, J. Colloid Interface Sci. 287 (2005) 25–34.
[19] S. Meenakshi, N. Viswanathan, Identification of selective ion exchange resin for fluoride sorption, J. Colloid Interface Sci. 308 (2007) 438–450.
[20] M.H. Zhu, Instrumental Analysis, Higher Education Press, Beijing, 2000.
[21] J.X. Xie, J.B. Chang, X.M. Wang, Applications of Infrared Spectroscopy in Organic and Pharmaceutical Chemistry, Science Press, Beijing, 2001.
[22] Z.L. Wang, S.W. Lin, Y.M. Lu, Study of absorption equilibrium and kinetics of L-tyrosine on 732 cation-exchange resin in a batch adsorber, Ion exch. Adsor. 24 (2008) 55–63.
[23] F. Wang, L.J. Wang, J.S. Li, X.Y. Sun, Y.P. Han, Adsorption properties of Pb(II)ions on a macroporous weakly acidic cation exchange resin, J. Beijing Univ. Chem. Technol. 36 (2009) 23–27.
[24] F. Gode, E. Pehlivan, Adsorption of Cr(III) ions by Turkish brown coals, Fuel Process. Technol. 86 (2005) 875–884.
[25] S. Rengaraj, C.K. Joo, Y. Kim, J. Yi, Kinetics of removal of chromium from water electronic process wastewater by ion exchange resins: 1500H and IRN97H, J. Hazard. Mater. B 102 (2003) 257–275.
[26] A. Sari, M. Tuzen, D. Citak, M. Soylak, Equilibrium, kinetic and thermodynamic studies of adsorption of Pb(II) from aqueous solution onto Turkish kaolinite clay, J. Hazard. Mater. 149 (2007) 283–291.
[27] Z.J. Wu, H. Joo, K. Lee, Kinetics and thermodynamics of the organic dye adsorption on the mesoporous hybrid xerogel, Chem. Eng. J. 112 (2005) 227–236.
[28] F.C. Wu, R.L. Tseng, S.C. Huang, R.S. Juang, Characteristics of pseudo-second-order kinetic model for liquid-phase adsorption: a mini-review, Chem. Eng. J. 151 (2009) 1–9.